Journal of Optoelectronics and Advanced Materials Vol. 7, No. 5, October 2005, p. 2501 - 2506

DEPOLLUTION EXPERIMENTS WITH REPETITIVE PULSED CORONA PLASMAS

N. Georgescu*, R. Minea, C. P. Lungu

National Institute for Lasers, Plasma and Radiation Physics, Magurele-Bucharest, Romania

Nitrogen oxide (NO) and sulfur dioxide (SO_2) are some of the most difficult air pollutants to remove chemically. However, it has been shown to decompose them by electrical discharges. In this work, the effect of reactor geometries (point-plate, wire-plate, wire-cylinder) on NO and SO_2 decomposition in pulsed corona plasmas is examined. The wire-cylinder geometry is the optimum one. A simulated polluted air was treated with pulsed corona plasmas in a wire-cylinder reactor. By using ethanol as additive, and γ-alumina as catalyst, an energy efficiency of 18.7 eV / (NO_X molecule), for 82 % reduction ratio, was obtained. The main electronically-chemical reactions implied in the pollutants destruction are then discussed.

(Received February 25, 2005; accepted September 22, 2005)

Keywords: Gases pollution control, Corona plasmas, Repetitive high-voltage pulses

1. Introduction

The method of pulsed corona induced plasma chemical process, introduced by Masuda [1] was proved to be competitive and promising by many research works [2, 3] as dry method for desulphurization and has many merits, such as removing SO_2 and NO simultaneously.

The corona plasmas are produced in a reactor chamber, between two or more electrodes, by applying between them pulsed electrical voltages. The inter-electrodes space is used to "treat" the polluted gas with the corona electrons. The pulsed corona plasmas have some important advantages over the DC ones. If the electrical pulses have less than 1 μs width, much higher electric fields can be applied, without causing spark breakdown in the reactor. The higher electric fields generate electron concentrations of order of magnitudes larger than under DC conditions. Because of the higher concentrations, space charge effects disperse electrons more uniformly throughout the reactor volume. The reactors can be thus designed with larger volumes, and this means a greater productivity of the depollution process. Also, for short corona pulses, the formed ions have a low temperature, and this means that less energy is lost for the gas heating. In this way, greater energy efficiencies may be obtained.

The energy efficiency is the energy required to destroy a pollutant molecule. The best result we know at this moment is an energy efficiency of 20.4 eV / (NO_X molecule), for 60 % reduction ratio [4]. The "NO_X" gas means the mixture of NO and NO_2 molecules.

The energy efficiency for a reactor chamber is defined as:

$$\varepsilon = W / \Delta N, \tag{1}$$

where W is the energy dissipated by corona effect, and ΔN is the number of the destroyed pollutant molecules. W is given by:

$$W = w \ f \ t_R = w \ f \ V_R / q, \tag{2}$$

* Corresponding author: ngeorge@infim.ro

with w - the energy dissipated per pulse by corona effect; f - the pulse repetition frequency; t_R - the gas residence time in the reactor chamber; V_R - the volume of the reactor chamber; q - the gas flow rate. Also,

$$\Delta N = N_{GAS}\ \Delta c = n_{GAS}\ V_R\ \Delta c, \tag{3}$$

where n_{GAS} is the molecules density of the polluted gas, and Δc is the reduction of the concentration of the pollutant molecules, relative to the polluted gas molecules. For Normal Pressure and Temperature (NPT), $n_{GAS} = 2.505 \cdot 10^{25}$ molecules / m^3 . A practical expression for ε results if w is given in [mJ/pulse], f - in [pulses per second], q - in [liters/min], Δc - in parts per million [ppm], ε - in [eV/molecule]:

$$\varepsilon = 14.97\ w\ f\ /\ (q\ \Delta c) \tag{4}$$

Each geometry of the reactor chamber has a given value for ε. For greater Δc, greater energies dissipated per pulse by corona effect must be realized. That is why w is one of the main parameters we have in view, when the various geometries are compared.

2. Experimental set-up

For gas treatment with repetitive pulsed corona plasmas, a depollution system has been carried out. Its main sub-systems are: 1. High-voltage repetitive pulser; 2. Reactor (depollution) chamber; 3. Gas flow circuit; 4. Gas analyzer.

2.1 High-voltage repetitive pulser

The high-voltage repetitive pulser discharges a capacitor in the primary of a pulse transformer. The high voltage switch is a TGI1000/25 thyratron (25 kV, 1 kA maximum, 1 A average). The capacitor is resonantly charged in the inter-pulses interval, by using a high voltage rectifier, and an inductance-diode circuit. The pulse transformer is the key component of this subsystem. It must assure a very good magnetic coupling between the primary and the secondary winding. Many construction solutions have been tested. The best solution is a transformer with 5 - 10 parallel wires, wound together on a toroidal magnetic core. Two types of magnetic core material are used: a. Amorphous magnetic material (Metglass 2605CO - Allied Signal Inc. - USA). The core is made of strip with 25 mm width and 23 microns thickness, having 4 microns of interlaminar insulation. The core dimensions are: 172 mm outer diameter, 110 mm inner diameter, 25 mm height. b. Ferrite type material. The toroidal core dimensions are: 90 mm outer diameter, 70 mm inner diameter, 40 mm height. With 25 turns windings, high-voltage pulses with 25 - 100 ns rise-time have been obtained. The rise-time value depends of the winding connection structure, and also of the transformer ratio (1:2, or 1:3).

By using the described pulser, electrical pulses with tens of kV amplitude, tens up to hundreds of ns width, tens up to hundreds of A load current are obtained. The repetition frequency can be varied between 0 - 1000 pulses per second.

The voltage pulses are measured with a capacitive-resistive divider (Tektronix, model P6015), with division ratio 1/1000. Rise times in excess of 10 ns are correctly measured. For current pulses, Tektronix P6021 probe with passive termination is used. In this case, the bandwidth is 120 Hz - 60 MHz. The voltage and current probes are both connected to a digital oscilloscope: Tektronix TDS 3012, or Tektronix TDS 1012 (100 MHz bandwidth for both).

2.2 Reactor chamber

2.2.1. Point-plate geometry. A structure with 5 needle-electrodes has been used. The 5 needle electrodes are uniformly spaced on a circumference with 15 mm diameter. The plane electrode is a 20 mm diameter disk. The inter-electrodes distance (d) can be varied up to 100 mm.

All the structure is mounted in a cylindrical glass chamber, 30 mm internal diameter. The active volume of the reactor chamber depends on the inter-electrodes distance. If this distance is 20 mm, then the reactor volume is of 15 cm^3.

2.2.2. Wire-plate geometry. A stainless steel wire ($2r$ = 0.5 mm diameter) is mounted above the plane electrode. The wire-plane distance (d) can be 10, 20, 30, 40 mm. The structure length is of 400 mm, the same as in the wire-cylinder geometry. In order to eliminate the edge effects, the plane electrode has 300 mm width. For d = 20 mm, the reactor volume is of 320 cm^3.

2.2.3. Wire - cylinder geometry (Fig. 1). The central electrode is made of stainless steel (2r = 0.5 mm diameter). The outer electrode (made also of stainless steel) is a cylinder with $2R$ = 43 mm inner diameter. The chamber length – 400 mm – means an internal volume of 580 cm^3.

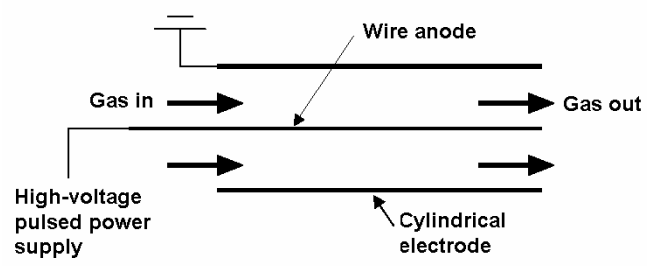

Fig.10. The wire-cylinder geometry principle.

2.3 Gas flow circuit

The first experiments were performed with dry/humid air streams. Then we used a mixture of N_2 with 500 parts per million (ppm) NO and 1000 ppm SO_2 (made by SIAD S.p.A - Italy). Finally, by adding oxygen in this mixture, a polluted air was simulated. The gas streams pass through flow controller devices made with Cole-Parmer tube flowmeters and with inserted valve cartridges. Flow rates of up to 10 l/min can be controlled and measured. The gas mixture may be humidified by passing it through water, possibly containing an additive. After the humidifier, the gas mixture enters the reactor chamber. The treated gas enters in the detection box, either directly, or after passing through a catalyst.

2.4 Gas analyzer

A gas analyzer (KM9106 - Kane Intnl. Ltd. - England) with electro-chemical sensors was used to measure concentrations of NO, NO_2, SO_2, CO, O_2. The analyzer probe also measured the gas temperature (up to 650^O C). Data was sent to a remote handset through the connection lead to be stored. All logged information was displayed on the handset, downloaded to a computer (with the FIREWORKS software) or output directly to an internal printer.

3. Experimental Results

To compare the different geometries, the applied voltage $v(t)$, and the corresponding pulsed current $i(t)$ are being measured. The following parameters are being calculated: electrical charge per pulse; density of the corona electrons; energy dissipation by corona effect.

The electrical charge per pulse (Q_{PULSE}) is obtained by integrating the corona current in time variable. The corona current pulse ($i_C(t)$) is given by:

$$i_C(t) = i(t) - i_D(t) = i(t) - C\ dv/dt, \tag{5}$$

where $i_D(t)$ is the displacement current, and C is the capacitance of the reactor chamber. It must be mentioned that the displacement current is much less than the total pulsed current. In the wire-

cylinder geometry, C = 5 pF only, and $i_D(t)$max = 1 A, for the case when the maximum value of the total pulsed current is of 56 A. In the other geometries, the reactor chamber capacitance has much smaller values. Consequently, the displacement current keeps on being much less than the total pulsed current. Therefore, with a very good approximation, the measured pulsed currents are the corona current ones. With the electrical charge per pulse (Q_{PULSE}), the density of the corona electrons (n_{EL}) is obtained. Finally, the energy dissipation by corona effect (w) is calculated as the time integral of the $v(t)\cdot i_C(t)$ product.

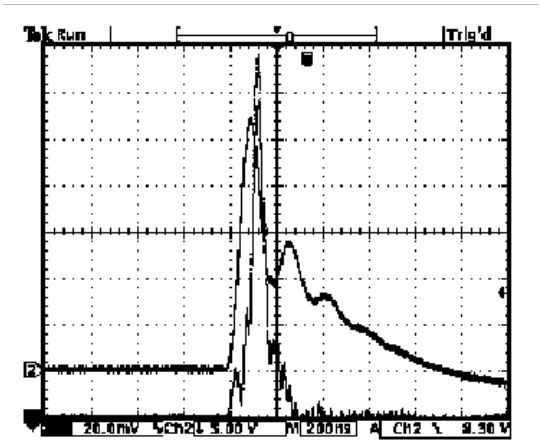

Fig. 2. Point-plate geometry: The applied voltage (2) and the corona current pulse (1) (5 kV/div; 200mA/div; 200 ns/div., d = 20 mm; V_R = 15 cm^3). Reactor chamber with humid air stream.

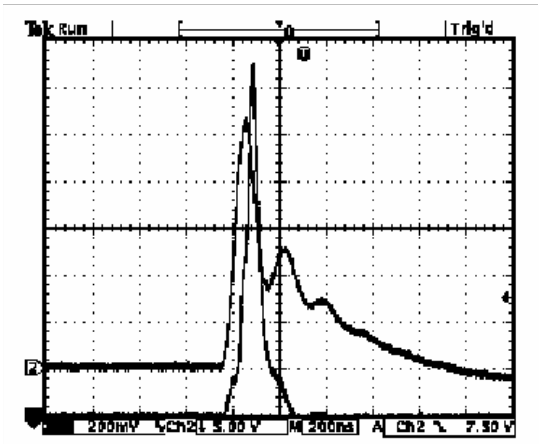

Fig. 3. Wire-plate geometry: The applied voltage (2) and the corona current pulse (1) (5 kV/div; 2A/div; 200 ns/div., r = 0.25 mm; d = 20 mm; V_R = 320 cm^3). Reactor chamber with humid air stream.

Figs. 2 – 4 present typical examples of the applied inter-electrodes voltage and the corona current pulse for the three different geometries of the reactor chamber. In all cases, the maximum inter-electrodes voltage is of 27 kV, and the positive corona effect is produced.

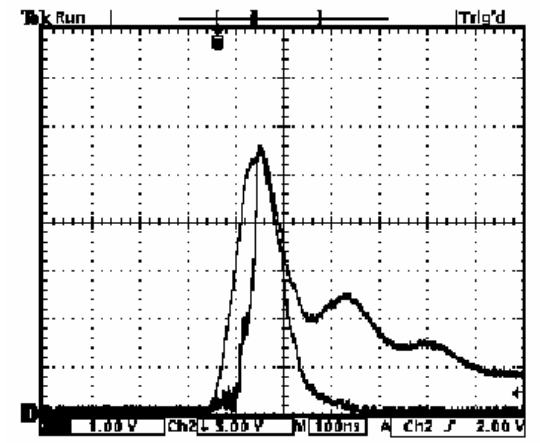

Fig. 4. Wire-cylinder geometry: The applied voltage and, within it, the corona current pulse (5 kV/div; 10 A/div; 100 ns/div. r = 0.25 mm; R = 21.5 mm; V_R = 580 cm^3). Reactor chamber with humid air stream.

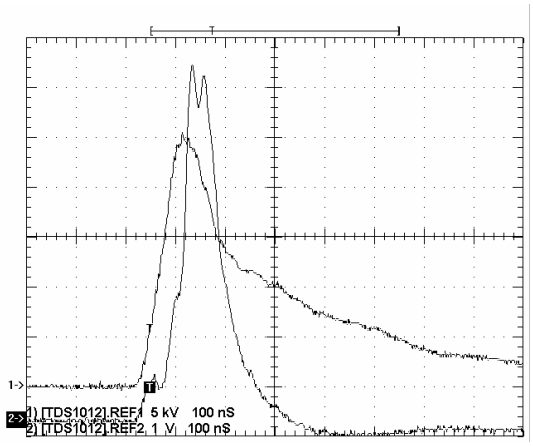

Fig. 5. Wire-cylinder geometry: The applied voltage (1) and the corona current pulse (2) (5 kV/div; 10 A/div; 100 ns/div. r = 0.25 mm; R = 21.5 mm; V_R = 580 cm^3). Reactor chamber with simulated polluted air, combined with ethanol molecules.

In Fig. 2, for a point-plate geometry (20 mm interelectrodes distance, 15 cm^3 the reactor volume), the maximum corona current is relatively low - 1.56 A. However, because of the small reactor volume, the mean density of the corona electrons has the greatest value: $6.6 \cdot 10^{10}$ electrons/cm^3. But this value must be considered together with the residence time of the gas in the

reactor chamber - 0.5 seconds only, for 2 l/min flow rate. This means a low energy efficiency of the depollution process. Another disadvantage is the great spatial non-uniformity of the corona electrons.

Fig. 3 presents the results for the wire-plate geometry, with inter-electrodes distance of 20 mm. The maximum corona current is of 14.8 A. The density of the corona electrons is of $2.9 \cdot 10^{10}$ cm^{-3}. The gas residence time in the reactor chamber has a rather acceptable value: 10 seconds, for the same gas flow rate as in the point-plate geometry. Structures with more wires between parallel plates might be used [5], but mechanical construction problems may be rather difficult.

The wire-cylinder geometry gives the best set of results. In Fig. 4, the maximum current is of 56 A, meaning a corona electrons density of $5.4 \cdot 10^{10}$ cm^{-3}. The residence time is of 18 seconds, and the energy dissipated by corona effect is of 85 mJ per pulse. In the same time, there is a good spatial distribution of the corona electrons inside the reactor chamber. All these considerations led us to the conclusion that the wire-cylinder geometry is the optimum one.

Figs. 2 – 4 correspond to the first experiments, with air streams. In the next experiments, the mixture of (N_2 + 500 ppm NO + 1000 ppm SO_2) was used. With the wire-cylinder geometry, the energy dissipated per pulse by corona effect was greater than 100 mJ. For a pulse repetition frequency f = 20 pulses per second, and a gas flow rate q = 2 l/min, the NO concentration decreased by Δc = 260 ppm. Taking into account these values, the energy efficiency is less than 60 eV per NO molecule, for 52 % reduction ratio.

For better energy efficiencies, a more complex treatment was used: pulsed corona plasma, combined with an additive (ethanol), and with a catalyst (γ-alumina). In these experiments, a polluted air was simulated: the SIAD mixture (N_2 + 500 ppm NO + 1000 ppm SO_2), with a flow rate of 3.2 l/min, was combined with 0.8 l/min oxygen flow. The resulting gas mixture was (80 % N_2 + 20 % O_2 + 400 ppm NO + 800 ppm SO_2). N_2 and O_2 have about the same concentration as in air. This simulated polluted air is passed first through a solution of 20 % ethanol in water. The mixture is then treated with pulsed corona plasma, in the reactor chamber. Figure 5 presents the applied inter-electrodes voltage and the corona current pulse for the described experimental conditions. For an inter-electrodes voltage of 25 kV maximum, the maximum corona current is of 70 A. The energy dissipated by corona effect is of 100 mJ per pulse. The pulse repetition frequency was of 20 pulses per second.

After the pulsed corona treatment, the gas was passed through a catalyst: spherical pellets (2 – 3 mm diameter) of porous γ-alumina (5 m^2/g).

By using this complex treatment, the following energy efficiencies were obtained:

- 18.7 eV / (NO_X molecule), for 82 % reduction ratio. This energy efficiency is better than the best result we know at this moment: 20.4 eV / (NO_X molecule), for 60 % reduction ratio [4].
- 11.0 eV / (SO_2 molecule), for 85 % reduction ratio.

4. Discussion

The reduction of NO and SO_2 with repetitive pulsed corona plasmas is a complex reaction that can be the result of several parallel and/or consecutive reaction steps. Different reaction mechanisms have been proposed for this reaction, which can be roughly classified into two general categories: the "decomposition mechanism" and the "reduction mechanism"[6]. The former mechanism implies decomposition by electron impact reactions and the latter one considers that the reduction of NO into N_2 and SO_2 into H_2SO_4 take place via the formation of nitrogen and oxygen containing intermediates, and it has been reported by other researchers [7].

We may expect the following processes based on the results and literature. During the initial current pulse period [0 – 100 ns], electron impact reactions produce radicals. Important electron impact reactions include:

$$e + N_2 \rightarrow N + N + e \quad (6)$$

$$e + NO \rightarrow N + O + e \quad (7)$$

$$e + H_2O \rightarrow OH + H + e \quad (8)$$

The effective removal of NO and SO_2 can be assumed by following reactions:

$$NO + N \rightarrow N_2 + O \quad (9)$$

$$NO + O + M \rightarrow NO_2 + M \quad (10)$$

$$NO_2 + OH + M \rightarrow HNO_3 + M \quad (11)$$

$$SO_2 + OH + M \rightarrow HSO_3 + M \quad (12)$$

$$HSO_3 + O_2 \rightarrow SO_3 + HO_2 \quad (13)$$

$$SO_3 + H_2O \rightarrow H_2SO_4 \quad (14)$$

Reaction (9) is a reduction one being the most preferred with respect to the larger reaction rate compared with the reactions rates of the oxidations channels (10) – (14) [8, 9].

$$k_4 = 3.41\times10^{-11}\exp\left(-\frac{24}{T}\right) \quad [\,cm^3\,s^{-1}\,] \quad (15)$$

The oxidation reaction (11) is controlled by OH radical produced by H_2O vapor decomposition (reaction (8)) and NO_2 formed following reaction (10). Also OH formation is important for the SO_2 conversion to SO_3 (reactions (12), (13)) then SO_3 fast react with water vapors (reaction (14)) to produce H_2SO_4.

Depending on the nature of the NO/SO_2 source, different channels may be preferred for plasma depollution. For sources such as coal-fired power plants, production of HNO_3 could be an acceptable option, since the effluent can be treated with base solutions to produce salts and water which then can be easily removed. For automobile applications, reaction (9) is more favorable as the harmful gas is converted into pure N_2 and O_2 ($O + O \rightarrow O_2$).

5. Conclusions

We examined the depollution of gas mixtures by using point-plate, wire-plate, and wire-cylinder geometries. The wire-cylinder geometry is the optimum one. With this optimum gometry, by using ethanol as additive, and γ-alumina as catalyst, an energy efficiency of 18.7 eV / (NO_X molecule), for 82 % reduction ratio, was obtained. The treated gas was a simulated polluted air. The energy efficiency is better than the best result we know at this moment. The presented results indicate that NO is decomposed into N_2 and O_2. Possible oxidations reactions lead to formation of HNO_3 and H_2SO_4, products that can be easily removed from the system.

References

[1] S. Masuda, Y. Wu, Institute of Physics Conference, Oxford, 1987, p. 249.
[2] Y. Wu, J. Li, N. Wang, G. Li, J. of Electrostatics **57**, 233, (2003).
[3] W. Niessen, O. Wolf, R. Schruft, M. Neiger, J. Phys. D: Appl. Phys. **31**, 542, (1998).
[4] M. Dors, J. Mizeraczyk, Catalysis Today **89**, 127, (2004).
[5] D. Wang, K. Fujiya, T. Namihira, S. Katsuki, H. Akiyama, Proc.14th IEEE International Pulsed Power Conference, Dallas, TX, USA, 2003, p. 1270.
[6] G. E. Marnellos., E. A. Efthimiadis, I. A. Vasalos, Appl. Catalysis B: Environmental **48**, 1, (2004)
[7] V. I. Parvulescu, P. Grange, B. Delmon, Catal.Today **46**, 233, (1998).
[8] B. Eliasson, U. Kogelschatz, IEEE Trans. On Plasma Science **19**, 1065, (1991).
[9] R. Dorai, Master Thesis, Graduate College of the University of Illinois at Urbana-Champaign, (2000).